Supplementary Methods

BAC isolation and characterization

The human hBAC clone (RPL11-997L11) encompassing the entire IL-8 gene, was grown in LB agar supplemented with 25 μg/ml of chloramphenicol (Sigma, MO) at 30^0C. Four individual colonies were picked for BAC plasmid isolation using a Nucleobond kit (Qiagen, CA). These BAC plasmids were analyzed for their integrity by restriction analysis and electrophoresis (data not shown).

To ascertain proper IL-8 gene splicing in mouse cells, each BAC plasmid (20 μg) was co-transfected with GFP-expressing vector (pMIG, 2 μg) into mouse dendritic DC2.4 cells using Lipofectamine 2000. Twenty-four hours later, the transfected cells were checked for transfection efficiency by analysis of GFP expression. Cells were then treated with 50 ng/ml of mouse IL-1beta for 2 hours or left untreated. Total RNA was isolated from transfected cells using Trizol reagent (Invitrogen), reverse transcribed (RT) using the Superscript III kit, (Invitrogen) and PCR amplified using IL-8-specific primers located in different exons. One hBAC plasmid had the properly spliced PCR fragment of the IL-8 gene and this was used for FISH analysis of hBAC complexity/ integrity with normal human blood cells. This analysis unambiguously linked the chosen hBAC to a unique site corresponding to the known IL-8 gene location in the q13.3 band of human chromosome 4 (data not shown). Transgenic mice (CBA/C57BL/6) bearing IL-8 hBAC were generated in Transgenic Core Facility of Columbia University. Three pairs of hBAC-specific primers that amplified 500-600 bp fragments from different parts of hBAC plasmid were used to identify hBAC-positive transgenic pups by PCR analysis.

Inflammation-associated colonic carcinogenesis.

Colonic tumorigenesis was induced in transgenic IL-8 mice and their wild type littermates as described previously [32]. Eight week old mice were treated with a single dose of azoxymethane (AOM) (10 mg/kg i.p.) followed by 3% DSS in the drinking water beginning one week later. In tumor bearing mice, twenty weeks following AOM, mice were sacrificed and the colon, spleen, bone marrow and peripheral blood analyzed. The colons were removed, opened longitudinally and analyzed for the presence of macroscopically visible tumors. Colonic tissues were fixed with formalin and paraffin embedded or processed for RNA extraction and expression analysis (see below for details). Histologic sections were prepared and stained with hematoxylin and eosin (H&E) or various antibodies as indicated. H&E stained slides were examined for inflammation and the presence of neoplastic or pre-neoplastic lesions using light microscopy.

APCmin model of small intestinal adenomas

To examine the effects of IL-8 on the spontaneous development of small intestinal adenomas, IL-8 transgenic mice were crossed to *APCmin*+/- mice that are known to develop intestinal adenomas following loss of heterozygosity. At 16 weeks of age, mice were sacrificed, the small intestine removed and cut along the midline, and the number of adenomas enumerated. Tumor burden of IL-8 x *APCmin*+/- mice was then compared to age-matched *APCmin*+/- controls. Splenic IMCs were also quantified from the mice examined using FACS as described below.

Two mouse models of gastric carcinogenesis

IL-8 transgenic mice or age-matched WT control mice were infected with *H. felis* as previously described (0.2 ml in trypticase broth) by oral gavage three times per week

every other day for a total dose of 100 million colony-forming units per mouse treatment as previously described [33]. Additionally, to investigate the role of IL-8 in second model of gastric cancer, we crossed IL-8 mice (line #176) with INS-GAS mice (FVB background), that previously have been reported to develop spontaneous gastric cancer in the setting of elevated gastrin levels [34].

Histologic tissue preparation and immunohistochemistry

Colonic, gastric or tumor tissues were fixed in 10% formalin, embedded in paraffin, and processed by standard histological methods. Hematoxylin and eosin stained sections were prepared for histologic assessment of the respective tissues and histopathologic scores in stomach tissues were graded according to previously described criteria [38,39] by a pathologist blinded to treatment groups. A composite colonic histopathological score encompassing the severity of inflammation, edema, crypt atrophy, epithelial defects, hyperplasia, and dysplasia was used to compare mice among various treatment groups.

To perform immunohistochemical staining, 5 um serial sections were cut from each selected paraffin block. Immunohistochemical studies were performed with avidin–biotin–peroxidase complex kits (Vector Laboratories, Burlingame, CA, http://www.vectorlabs.com) according to the manufacturer's instructions. Primary antibodies (see below) and biotinylated secondary antibodies were diluted in 2% bovine serum albumin - PBS and incubated overnight at 4^{o}C or for one hour at room temperature respectively. Finally slides were counterstained with hematoxylin and mounted.

RNA isolation and quantitative RT-PCR analysis of gene expression.

Total RNA was extracted with Trizol reagent (Invitrogen, CA) and cDNA was synthesized from 4 μg of total RNA with Superscript III First Strand cDNA synthesis kit (Invitrogen, CA). Expression level of each gene was quantified by real-time RT-PCR assays using PCR conditions: 95 degrees for 15 minutes followed by 40 cycles of 94 degrees for 10 seconds, 55 degrees for 20 seconds and 72 degrees for 30 seconds using QuantiTect SYBR Green PCR kit (Qiagen) and 7300 Real Time PCR System (Applied Biosystems, CA). Primers used included: IL-8: CGTGGCTCTCTTGGCAGCCTTC (F), TCCACAACCCTCTGCACCCAGTT (R); CXCR-1: CCGTCATGGATGTCTACGTG (F), CAGCAGCAGGATACCACTGA (R); CXCR-2: ATCGACCGGGCTCTGGATGC (F), TGCTGTCTTTGGGCAGGGAGTC (R). Briefly, ΔCt was calculated by the subtraction of GAPDH Ct from the gene-specific Ct, and ΔΔCt was calculated by the subtraction of the gene-specific ΔCt from standard ΔCt (=40 cycles in this study).

Primary cell isolation, growth and stimulation.

Immature dendritic cells were prepared from mouse bone marrow as previously described [32], while macrophages were isolated from the peritoneum of thioglycolate treated mice. Cultures of both cell types were cultivated in basal RPMI-1640 or DMEM media supplemented with 10% low-endotoxin fetal bovine serum (Hyclone, Utah). Both cultures were then stimulated with 1-100 ng/ml of LPS (E.coli O5:B55; Sigma, MO). Gastric epithelial cells were removed using a crypt isolation technique [33], and then cultured as previously described [34]. Short-term colonic epithelial cell cultures were prepared as previously described [47].

FACS Analysis of spleen, bone marrow and circulating cells in acute inflammation and cancer

Whole bone marrow cells were flushed from both femurs and tibias of mice (WT and IL-8 transgenic) with Hanks' balanced salt solution (HBSS) containing 5% fetal bovine serum (FBS) (Gibco, Invitrogen, Carlsbad, CA). To obtain peripheral blood mononuclear cells, blood was drawn by percutaneous intracardiac puncture and mixed in ACD tubes (BD Falcon, Bedford, MA) for anti-coagulation. Red blood cells (RBC) were removed by RBC lysis buffer (BD Biosciences, San Jose, CA). To obtain splenocytes, spleens were ground on a 40-microm cell strainer (BD Falcon, Bedford, MA) and flushed with HBSS with 5% FBS (Gibco, Invitrogen, Carlsbad, CA). Cell pellets were resuspended with HBSS containing 5% FBS following centrifugation (Gibco, Invitrogen, Carlsbad, CA). Cells were diluted to a concentration of 1 million cells per 100 mL of HBSS containing 5% FBS (Gibco, Invitrogen, Carlsbad, CA) in 5ml FACS tubes (BD Falcon, Bedford, MA). Antibodies used in this study included: anti-CD11b (eBiosciences, San Diego, CA) and anti-Gr-1 antibody (BD Biosciences, San Jose, CA). 4',6-diamidino-2-phenylindole (DAPI) (DAKO, Glostrup, Denmark) was added at a concentration of 1/1000 to exclude dead cells. FACS was performed on BD LSR (BD Biosciences, San Jose, CA) and BD Aria cell sorters (BD Biosciences, San Jose, CA), and later analyzed using FlowJo 7.2.

Assessment of immature myeloid cell derived interleukin-8 on xenograft colonic tumor growth

To specifically assess the contribution of immune cell derived IL-8 on tumorigenesis, we performed xenograft studies using the CT-26 BALB/c mouse colon cancer cell line which does not express IL-8. CT-26 colon cancer cells (1.0×10^6 cells) were co-injected subcutaneously into the flank of NOD-SCID mice in combination with,

or without 1.2 x10^6 IMCs (CD11b+Gr-1+ cells) FACS sorted from the bone marrow of either IL-8 transgenic mice or WT mice. Xenograft tumors were examined every 2 days to monitor for changes in tumor size using calipers. At the end of 2 weeks, mice were sacrificed and tumor xenografts removed from the mouse by carefully dissecting the tumors from the overlaying skin. Tumors were then weighed and placed in 10% formalin for tissue fixation as described above.

In vitro cell migration assay

Whole bone marrow cells were flushed from both femurs and tibias of UBC-GFP transgenic (purchased from Jackson Labs, Bar Harbor, Maine) mice and CD11b+Gr1+ immature myeloid cells sorted from the bone marrow population using FACS as described above. CD11b+Gr1+ cells (0.5 x 10^6 cells) were then added to the top chamber of a 3 um pore size transwell filter (Costar) of a 6 well plate containing 1 ml of RPMI media containing 10% fetal bovine serum (Gibco, Invitrogen, Carlsbad, CA). Cells were then incubated for 24 h in the presence or absence of recombinant human IL-8 (100 ng/ml) that was added to the bottom chamber of the 6 well plate. The number of cells migrating across the transwell and visualized using phase microscopy was then expressed as the number of cells observed per high power field (HPF).

Colonic tumor microarray analysis

We aimed to identify the immune cells and molecules, that were induced or promoted by IL-8, but we had too little tumor sample to identify the cells by cell-sorting. Instead, we compared the genome-wide expression of IL-8 transgenic vs WT mice colonic tumors with Affymetrix Mouse 430.2 chips (n=3). Standard experimental and quality assessment methods were used [46]. Briefly, RNA was purified from colonic tumors of WT and IL-8

transgenic mice and cDNA synthesized using a One-cycle cDNA Synthesis kit (Affymetrix). cRNA was amplified with IVT MEGAscript® T7 Kit and hybridized with Genechip mouse genome 430 2.0 (Affymetrix). GCRMA was used to normalize the data [46,47]. Data was deposited in the Gene Expression Omnibus (GSE 39273) [46]. Limma [46] with empirical weights [48] was used to determine differential expression quantitatively. The gene expression barcode method [49, 50] was used to determine presence or absence of genes characteristic of particular immune cell types. We found 3 genes expressed in immune cells, which were expressed in all 3 IL8 transgenic mice but not in any of the controls: Ighm, Tsc22d3, and CX3CR**.** RT-PCR analysis of differential gene expression was performed to confirm the microarray results (Table 1)**.** Finally, we FACS sorted immune cell populations identified to as present or absent by the genes identified in the microarray analysis and confirmed that the gene(s) differentially expressed were indeed accurately reflective of the immune cells suggested by the Barcode.

Supplementary Figure Legends

Supplementary Figure 1.

Generation of a novel IL-8 expressing transgenic mouse model. (A) Schematic representation of the IL-8 containing BAC (not drawn to scale), with four exons shown as black boxes. The primer positions used for PCR-based genotyping are shown by arrows, with the size of amplified PCR fragments shown below. (B) FISH analysis showing the unique chromosome integration site of the BAC transgene of IL-8 transgenic mouse line #176. (C) Baseline complete blood count and differential of peripheral blood from WT and IL-8 Transgenic (Tg) mice. (D) Serum IL-8 levels in WT and IL-8 transgenic littermates injected with LPS. IL-8 levels in unchallenged mice (*black bars*) were below the assay detection limit. Founder lines and respective number of transgene copies (in brackets) are shown.

Supplementary Figure 2.

IL-8 accelerates colonic tumorigenesis in association with splenic hypertrophy. (A) Colonic tumor number (separated by size (< 0.5 cm or > 0.5 cm) in WT and IL-8 transgenic mice treated with AOM plus DSS (** $p<0.01$). (B) Expression of human IL-8 in colonic tumor tissues from AOM plus DSS treated IL-8 transgenic and WT mice as determined by ELISA (* $p<0.05$). (C) Assessment of colonic inflammation severity in H & E sections taken from WT or IL-8 transgenic mice treated with AOM and DSS. (D) Spleen size of colonic tumor bearing WT and IL-8 transgenic mice (* $p<0.05$). (E) Representative H & E microscopic images of spleens from WT and IL-8 transgenic

tumor-bearing mice. (F) Immunostaining of Ki67+ proliferating cells in crypts adjacent to AOM/DSS colonic tumors from WT and IL-8 transgenic mice. ($n \geq 4$ per group).

Supplementary Figure 3.

Expression of IL-8 accelerates the development of gastric inflammation and carcinogenesis during *long-term H. felis* infection. (A) H & E stained stomach sections from IL-8 transgenic and WT mice infected with *H. felis* at the indicated times. *Bars*, 100 μm (B) Summary of histological scores in mice infected with *Helicobacter felis* for 18 months. Each parameter was scored as previously described [1]. Data are expressed as the mean ± SEM. (C) Expression of human IL-8 (*a*) and human IL-8 mRNA (*b*) in gastric tissue from IL-8 transgenic and WT mice. Data are expressed as the mean ± SEM.

Supplementary Figure 4.

IL-8 expression accelerates gastrin-dependent gastric carcinogenesis. (A) Histologic score of invasive adenocarcinomas in INS-GAS/IL-8 and IL-8 mice at 12 months of age. (B) Gross appearance (*top*) and H&E stained sections (*bottom*) from INS-GAS/IL-8 and INS-GAS mice at 12 months of age. (*top*) *Bars*, 2mm (*bottom*) *Bars*, 100μm. (C) vWF immunostaining for quantification of microvessels with gastric tissue from INS-GAS/IL-8 and INS-GAS mice. (D) Expression of human IL-8 in gastric tissue from as measured by ELISA (left) and human IL-8 mRNA expression as determined by real-time qRT-PCR (right) in gastric tissue from INS-GAS/IL-8 and INS-GAS mice. Data are expressed as the mean ± SEM.

Supplementary Figure 5.

Secretion of hIL-8 by primary cultures of macrophages, dendritic cells and gastric epithelial cells isolated from transgenic mice. (A) IL-8 secreted in the culture supernatants of thioglycolate-induced peritoneal macrophages, bone marrow derived CD11c+ immature dendritic cells, and colonic epithelial cells isolated from WT or IL-8 transgenic mice and cultured in the presence or absence of LPS are shown. IL-8 chemokine levels (B), total number of nucleated cells (C) and myeloperoxidase (MPO) activity (D) in the peritoneal lavage of thioglycolate (4% i.p.) treated IL-8 transgenic mice versus WT mice are shown. (E) Pre-treatment with 100 μg i.p. anti-IL-8 antibody significantly inhibited mobilization of inflammatory cells into the peritoneum of thioglycolate treated IL-8 transgenic mice compared to IgG isotype control antibody treated mice. (F) Quantitative analysis of CD11b+Gr-1+ immature myeloid cells (left) and Ly6C+ and Ly6G+ myeloid cell subsets (right) mobilized into the peritoneal lavage of IL-8 transgenic versus WT mice 72 h following 4% thioglycolate injection (i.p.). (* $p<0.05$; ** $p<0.01$, *** $p<0.001$).

Supplementary Figure 6.

IL-8 enhances mobilization of immature myeloid cells in *APCmin*+/- mice and *in vitro*. (A) Quantitative analysis of splenic CD11b+ and Gr-1+ immature myeloid cells and (B) CD11bLy6C+ and CD11bLy6G+ myeloid cell subsets in IL-8/ *APCmin*+/- transgenic versus *APCmin*+/- tumor-bearing mice at 16 weeks of age ($n \geq 4$). (C) In vitro transwell migration of GFP labeled CD11b+Gr-1+ immature myeloid cells isolated from UBC-GFP transgenic mice and cultured in the presence or absence of IL-8 (100 ng/ml) or

LPS (5 ng/ml). (D) CXCR2 mRNA expression in Ly6C+ and/or Ly6C+ immature myeloid cell subsets sorted by FACS from the spleen of LPS-treated (5 mg/kg i.p.). (E) H&E staining of Ly6G+Ly6C+ versus Ly6G+Ly6C- myeloid cells sorted by FACS from LPS treated IL8Tg mice are shown. Black arrows denote Ly6G+Ly6C+ cells demonstrating the a circular ringed nucleus of immature myeloid, whereas red arrows point to more mature Ly6G+Ly6C- neutrophils displaying the characteristic polymorphonuclear structure.

Supplementary Figure 7.

IL-8 transgenic versus WT colonic tumor microarray analysis. (A) RT-PCR analysis of Ighm mRNA expression in various bone marrow derived immune cells showing Ighm expression predominantly within the CD220+ B cell population.

Suppl. Figure 1.

A

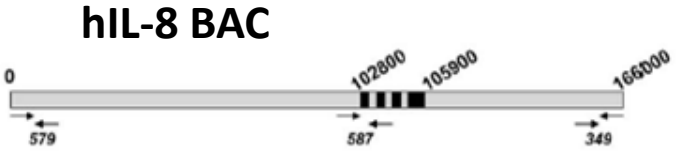

B

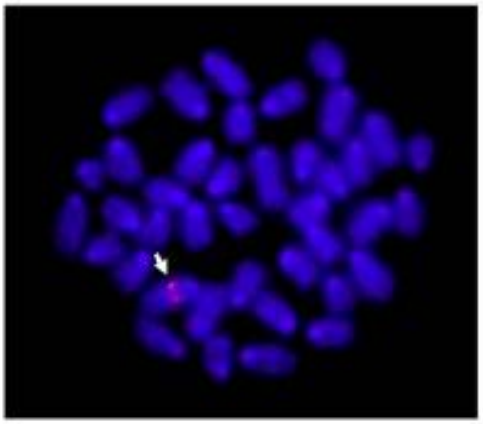

C

Count	WT		TgIL8
WBC (x10⁹/L)	12.4 +/- 2.9		11.8 +/- 1.0
Nϕ (% WBC)	17.8 +/- 3.8	=	20.3 +/- 2.5
RBC (x10¹²/L)	8.8 +/- 0.3		8.8 +/- 0.2
Platelets (x10¹²/L)	1.3 +/- 0.3		1.35 +/- 0.2

D

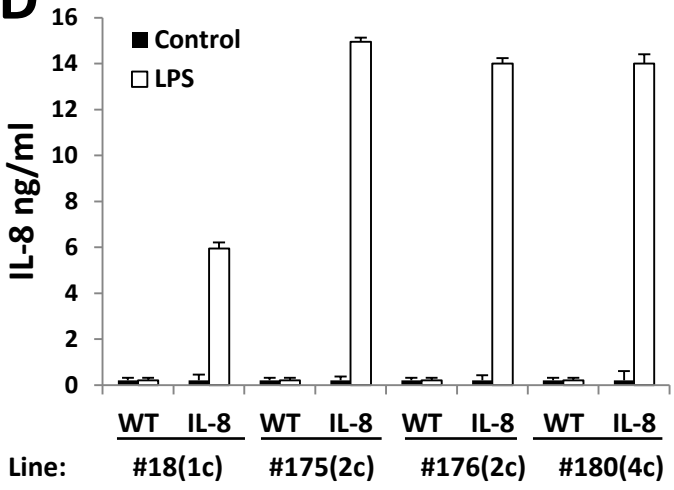

Suppl. Figure 2.

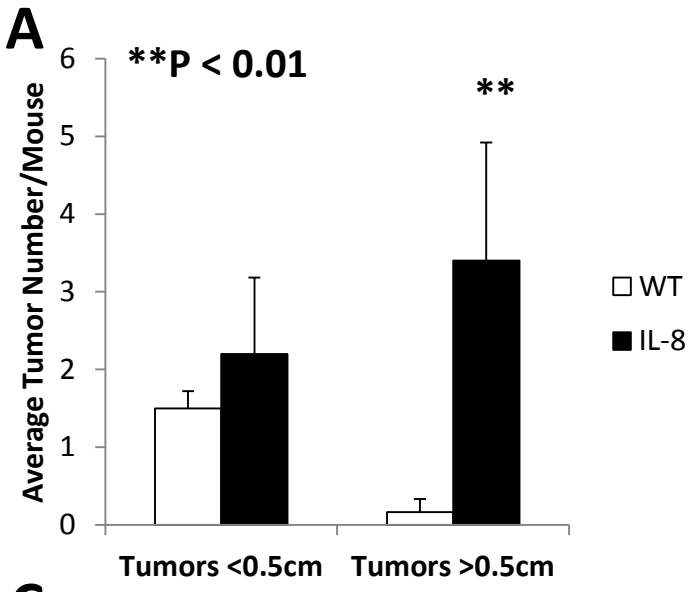

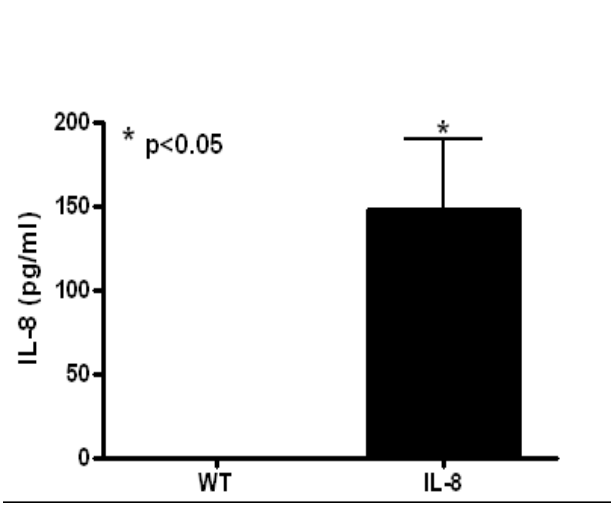

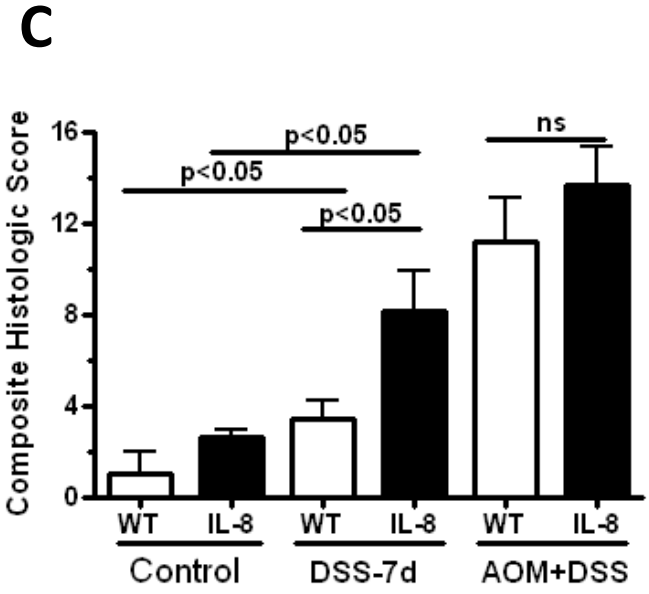

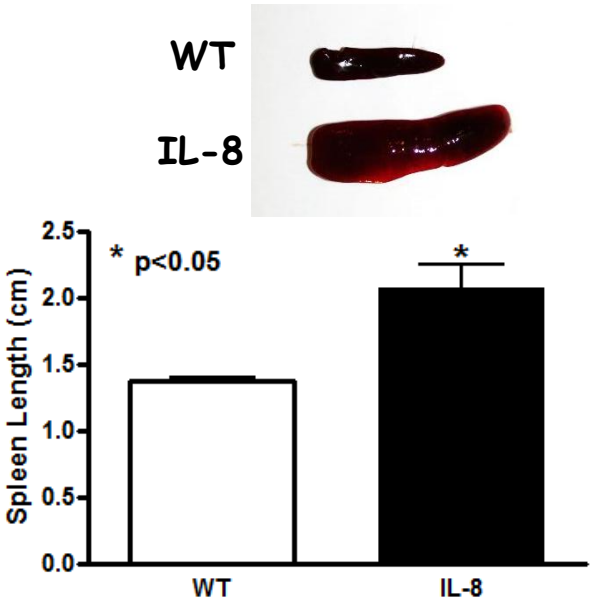

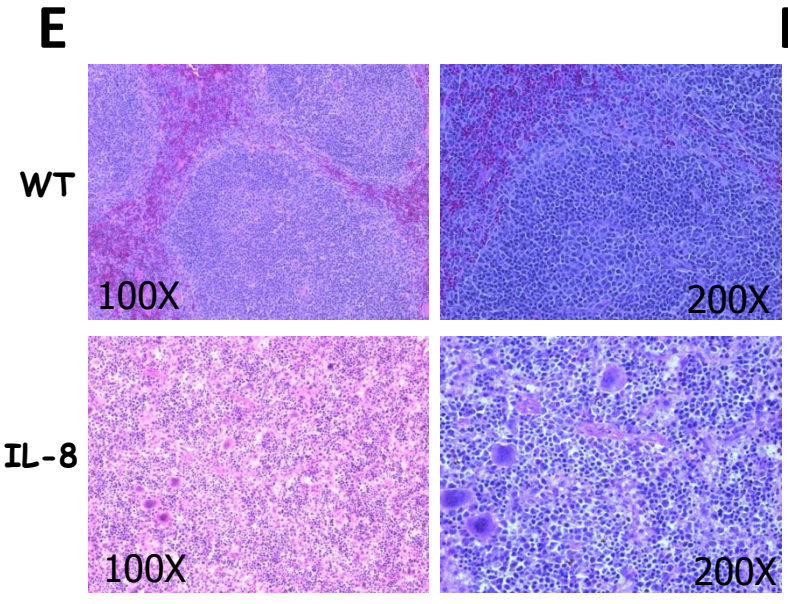

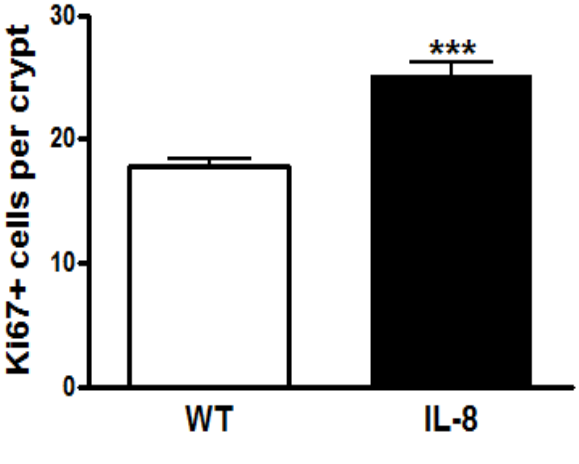

Suppl. Figure 3.

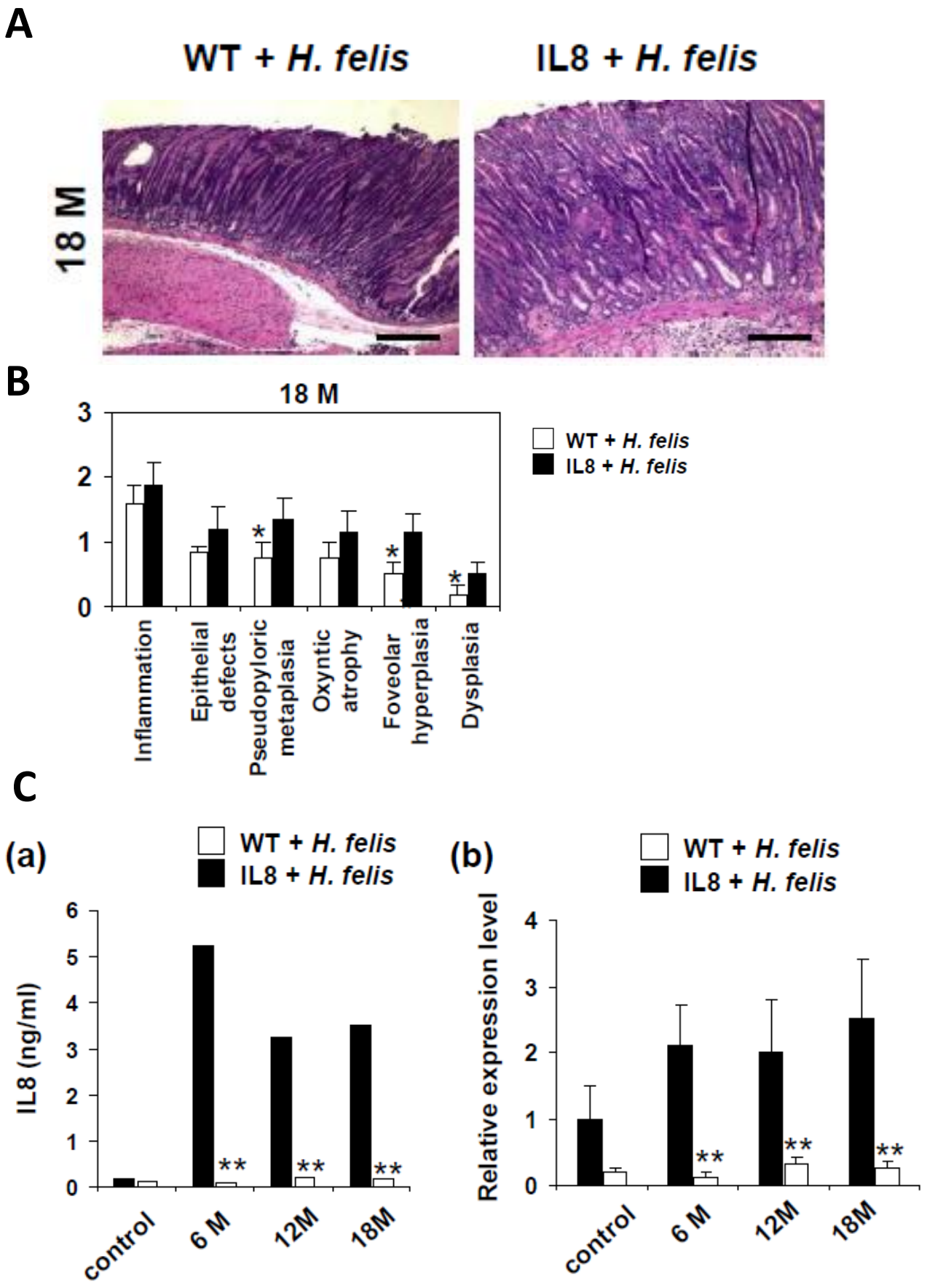

Suppl. Fig 4.

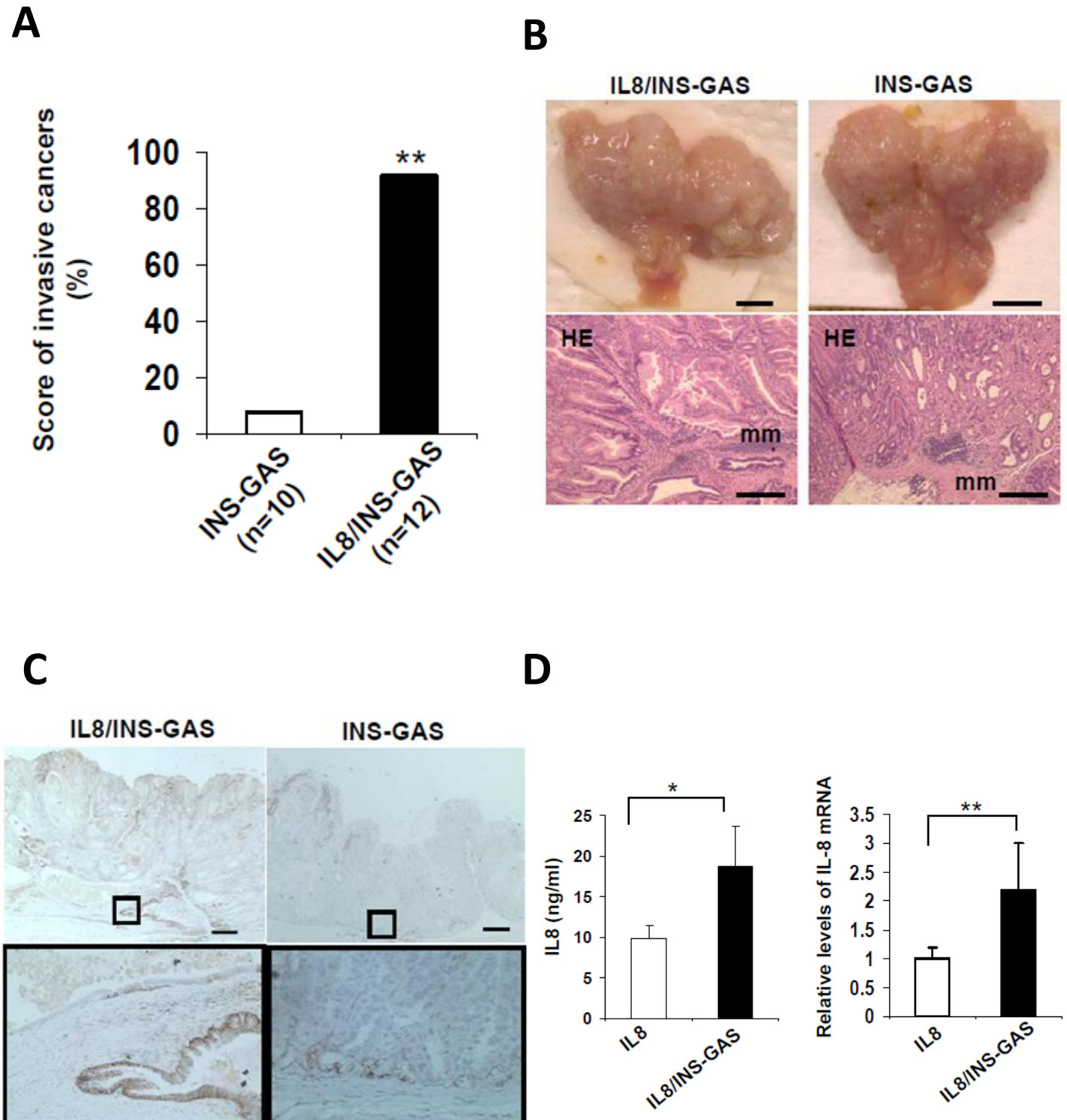
A
Score of invasive cancers (%)
100
80
60
40
20
0
**
INS-GAS (n=10)
IL8/INS-GAS (n=12)
B
IL8/INS-GAS
INS-GAS
HE
mm
HE
mm
C
IL8/INS-GAS
INS-GAS
D
IL8 (ng/ml)
25
20
15
10
5
0
*
IL8
IL8/INS-GAS
Relative levels of IL-8 mRNA
3.5
3
2.5
2
1.5
1
0.5
0
**
IL8
IL8/INS-GAS

Suppl. Figure 5.

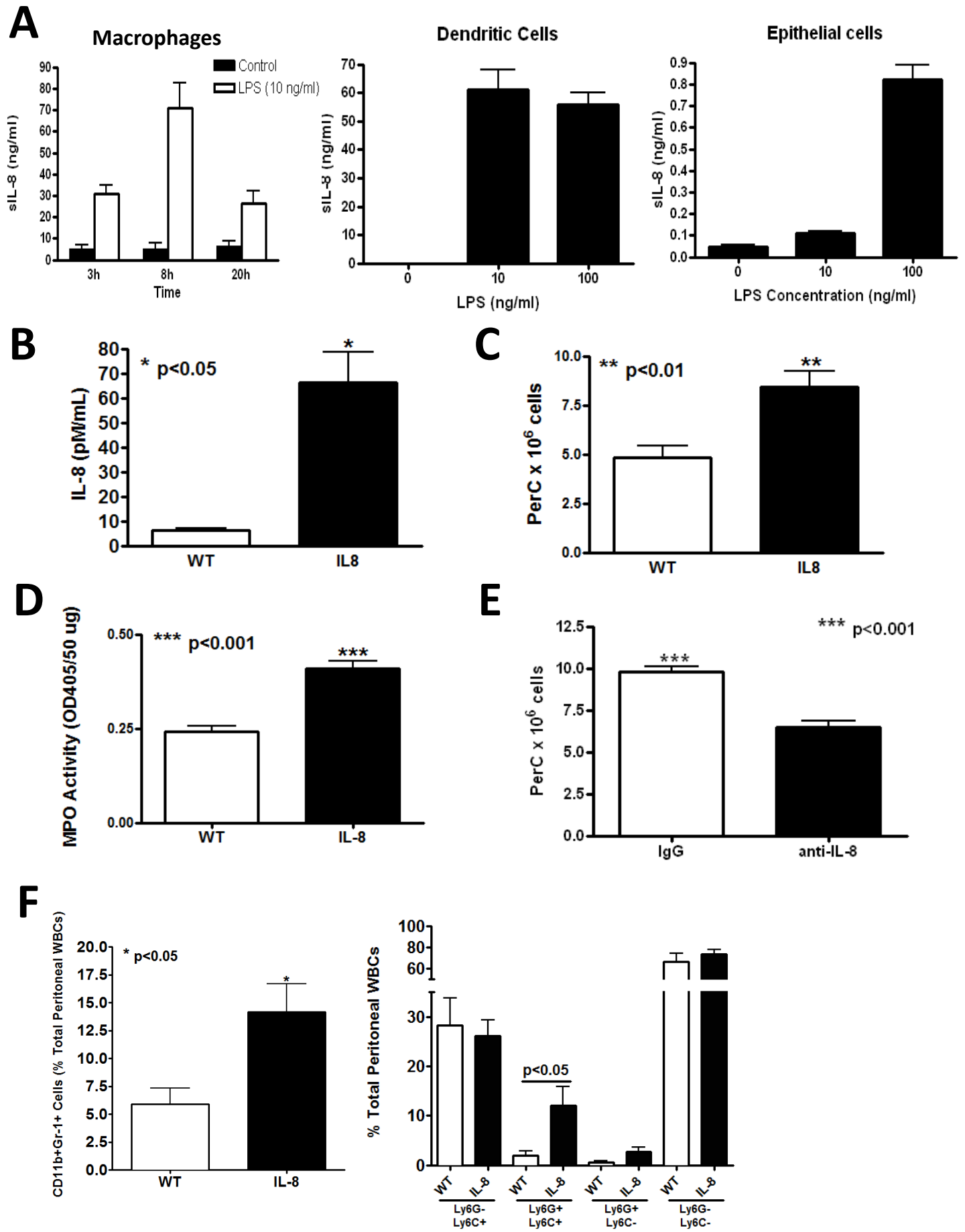

Suppl. Figure 6.

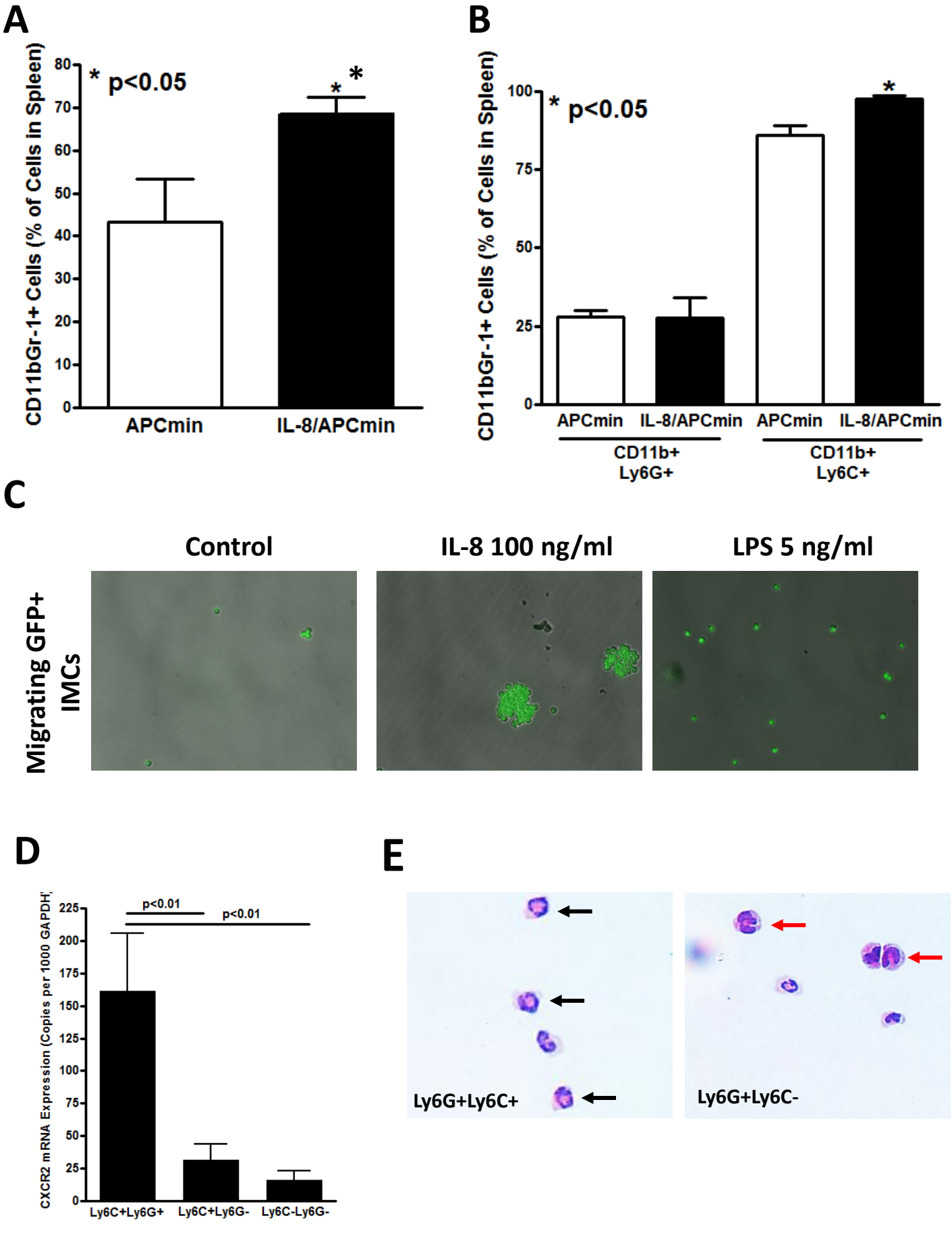

Suppl. Figure 7.

A